



LAWRENCE
LIVERMORE
NATIONAL
LABORATORY

Comparisons of Dense Plasma Focus Kinetic Simulations with Experimental Measurements

A. Schmidt, A. Link, D. Welch, J. Ellsworth, S.
Falabella, V. Tang

February 20, 2014

Physical Review E

Disclaimer

This document was prepared as an account of work sponsored by an agency of the United States government. Neither the United States government nor Lawrence Livermore National Security, LLC, nor any of their employees makes any warranty, expressed or implied, or assumes any legal liability or responsibility for the accuracy, completeness, or usefulness of any information, apparatus, product, or process disclosed, or represents that its use would not infringe privately owned rights. Reference herein to any specific commercial product, process, or service by trade name, trademark, manufacturer, or otherwise does not necessarily constitute or imply its endorsement, recommendation, or favoring by the United States government or Lawrence Livermore National Security, LLC. The views and opinions of authors expressed herein do not necessarily state or reflect those of the United States government or Lawrence Livermore National Security, LLC, and shall not be used for advertising or product endorsement purposes.

Comparisons of Dense Plasma Focus Kinetic Simulations with Experimental Measurements

A. Schmidt¹, A. Link¹, D. Welch², J. Ellsworth¹, S. Falabella¹, V. Tang¹

¹Lawrence Livermore National Laboratory

²Voss Scientific, LLC

Abstract

Dense plasma focus (DPF) Z-pinch devices are sources of copious high energy electrons and ions, x-rays, and neutrons. The mechanisms through which these physically simple devices generate such high-energy beams in a relatively short distance are not fully understood and past optimization efforts of these devices have been largely empirical. Previously we reported on the first fully kinetic simulations of a DPF and compared them with hybrid and fluid simulations of the same device. Here we present detailed comparisons between fully kinetic simulations and experimental data on a 1.2 kJ DPF with two electrode geometries, including neutron yield and ion beam energy distributions. A more intensive third calculation is presented which examines the effects of a fully detailed pulsed power driver model. We also compare simulated electromagnetic fluctuations with the first direct measurement of radiofrequency EM fluctuations in a DPF plasma. These comparisons indicate that the fully kinetic model captures the essential physics of these plasmas with high fidelity, and provide further evidence that anomalous resistivity in the plasma arises due to a kinetic instability near the lower hybrid frequency.

Introduction

We describe here three fully kinetic dense plasma focus (DPF) [1-4] simulations and compare their predictions in detail with a variety of measurements, some of which are the first of their kind. These simulations remain stable and energy-conserving through the entire Z-pinch phase, in which the plasma changes rapidly and exhibits high gradients. Modeling the entire Z-pinch phase – and thus counting all neutrons produced – is important for comparing yield predictions across different simulations. The production of a stable simulation for a specific configuration typically requires >100k cpu-hours. Here we compare simulated and experimentally measured neutron yields for two DPF gun geometries, demonstrating the model's ability to distinguish performance between similar gun designs. We additionally show a third calculation in which the boundary condition between electrodes is modeled using a pulsed power circuit, in order to include driver effects in the calculation. The simulations shown here reproduce experimentally measured ion beam energy distributions and radiofrequency fields in the plasma. This is the first comprehensive comparison of a fully kinetic model with these measured quantities in a DPF, demonstrating that the model can be used as a predictive design tool.

A DPF Z-pinch is a device consisting of two coaxially located electrodes with a high-voltage source at one end (Figure 1). In the presence of a low-pressure gas, the high-voltage source induces a surface flashover and the formation of a current-conducting plasma sheath across an insulator at the upstream end of the DPF. During the “run-down” phase, the current sheath is accelerated down the length of the electrodes by magnetic pressure, ionizing and sweeping up neutral gas as it accelerates. When the plasma sheath reaches the end of the inner electrode, a portion is pushed radially inward during the “run-in” phase. When the leading-edge of the current sheath reaches the axis, it “pinches” the plasma to create a hot, dense region that emits high-energy electron and ion beams, x-rays, and (in the presence of D or D-T) neutrons [4].

In addition to fluid modeling of DPFs, previous modeling work has included a non-self-consistent test particle approach to look at kinetic effects [5-9], kinetic simulations of a Z-pinch with scaled ion-electron mass ratio [10], and kinetic simulations of a conventional gas-puff Z-pinch [11]. We previously reported on the first fully kinetic model of a DPF Z-pinch device, including electrode boundaries, and demonstrated that a fully kinetic (both ions and electrons kinetic) approach is needed in order to see kinetic effects during the pinch phase, such as kinetic instabilities and beam formation [12]. Past measurements of DPF RF emission have been performed using microwave antennas in conjunction with band-pass waveguides that allowed various frequency bands to be transmitted [13].

Simulation and Experimental Set Up

The simulation set-up is detailed in [12] and is briefly summarized here: calculations were performed in the particle-in-cell (PIC) code large scale plasmas (Lsp) [14]. The time step was varied from 2.5×10^{-4} ns to 8×10^{-6} ns, and was reduced as the magnetic field in the simulation increased, ensuring the resolution of the electron cyclotron frequency. The calculation is initialized at the end of the run-down phase, with a 1-mm-width plasma sheath of uniform density. The neutral gas density in front of the sheath corresponds to 1 torr at STP, and the region behind the sheath is initially vacuum. The sheath density corresponds to a 10% sweep-up of neutral gas during the run-down.

Simulations are two dimensional in cylindrical coordinates (r, z). The two simulated electrode geometries shown in Figure 2 correspond to experimental geometries used on the existing 1.2 kJ DPF at LLNL [15]. The cathodes (outer electrodes) are represented by conducting boundaries at $r = 1.5$ cm and $r = 3.0$ cm for the two geometries. In the experiment, the cathode is not cylindrically symmetric, as it is a set of 8 rods arranged in a circular pattern. A 5-cm-long anode is represented by a conductive cylinder with outer radii of 1 cm and 1.5 cm for the two geometries. In the smaller geometry, the anode is hollowed out, while the larger geometry has only a small depression in the anode (Figure 2).

The voltage drive is modeled here in two ways. The first, and less computationally expensive, is with a prescribed incoming voltage wave traveling the length of the anode, with a reflected wave traveling back. The voltage is ramped up during the first 10 ns of the simulation (before the run-in), and then kept constant for the remainder of the simulation, resulting in a steady-state current of 180 kA and 200 kA, for the small and large guns respectively (Figure 3), before the pinch.

An additional simulation was run for the larger gun geometry which included the details of the driver characteristics, including capacitance, resistance, inductance, and line impedance. Using this driver model requires that the simulation run for ~ 450 ns of the circuit rise in addition to the ~ 160 ns of run-in and pinch (Figure 3). To keep the simulation manageably sized, the particles were initially placed at the end of the run-down and prevented from moving while the transmission line current rose nearly to its peak value. This method requires more computing time than the voltage wave method, but allows for self-consistent modeling of the plasma and drive after the particles are permitted to move.

While past DPF circuit models could predict the effect of driver characteristics on general plasma properties such as sheath speed, this model is the first to be able to self-consistently predict neutron yields including driver effects. Hereafter it can be used as a tool to predict and understand the performance for different drivers, such as the high impedance drivers that have empirically been shown to increase DPF neutron yield [16-18].

The ion energy distributions inside our DPF were measured with a time-of-flight (TOF) Faraday Cup diagnostic (Kimball Physics model FC-73A) located 65 cm from the pinch [15]. Neutron yields were measured with a Helium-3 neutron detector, calibrated with a Californium-252 source and accompanying MCNP calculations [15]. The electric field oscillations were measured using a small RF pick-up probe placed between cathode rods at the end of the anode, slightly inside the plasma. The RF probe was connected to a 12 Gs/s oscilloscope for measurement of oscillations up to 5 GHz.

Simulation and Experimental Results

The kinetic simulations shown here remain stable and energy-conserving through the entire pinch process so that a well-defined neutron yield could be obtained from specific electrode geometries (Figure 4). Repeated calculations with identical plasma conditions but different gridding or time-stepping exhibit a neutron yield variation of $\sim 10\%$. The kinetic calculations were able to differentiate neutron yield between the two similar DPF electrode geometries that we have tested experimentally. The two voltage wave driver simulations predicted a yield of 2.8×10^7 with the smaller gun geometry (measured yields are up to 4×10^7) and 1.6×10^7 with the larger gun geometry (measured yields are up to 2×10^7), despite the current being higher in the larger gun simulation. It is encouraging that the predicted yields for two similar guns are correctly ranked, though a simulated pressure scan must be done to confirm this prediction.

Including the driver characteristics at the anode-cathode boundary has the effect of decreasing the time over which neutrons are produced (Figure 4) and the overall yield. This result is expected since the real pulsed power system will not continue to provide a stiff voltage indefinitely. For the larger gun geometry with pulsed power circuit, a total yield of 6.9×10^6 was obtained, approximately half of the predicted yield when using the voltage wave driver. The neutron pulse was ~ 60 ns long with the voltage wave driver for both gun geometries and ~ 20 ns long with the pulsed power circuit. In both geometries, the simulations predict that the majority of neutrons are born in a region within 1 mm of the axis, and with an axial extent of ~ 1 cm and ~ 2.5 cm for the smaller and larger gun geometries, respectively (Figures 5a

and 5b). The predicted neutron birth region is shorter when the pulsed power circuit is included (Figure 5c).

Simulated and measured energy distributions of ion beams emitted from the DPF with smaller gun are shown in Figure 6. Measured energy distributions have been obtained from TOF Faraday cup measurements, which show significant signal above the noise for D^+ energies of 300 keV and below. The Faraday cup is on axis in front of the anode and its aperture subtends a 0.2 degree half-angle relative to the pinch. The simulated ion energy distribution was taken from a conic section with 22 degree half-angle for sufficient particle statistics. Substantial agreement between the simulated and measured distributions is found under 300 keV. The simulations additionally show a small population of ions with energies up to 1 MeV. Ion beams have been observed on a variety of DPFs with energies up to 8 MeV [19, 20], but MeV+ ions measured on other experiments are 1-3 orders of magnitude weaker in signal from 300 keV ions, and thus are not detectable with our experimental set up.

The frequency content of measured and simulated electromagnetic fields during the pinch for the larger gun geometry is shown in Figure 7. An EM pick-up probe positioned between cathode rods and connected to a high-bandwidth oscilloscope was used to measure EM oscillations in the plasma, up to 5 GHz. Figure 7a shows examples from both high and low quality pinches, as determined by the depth of the current dip and the neutron yield. Poor pinches did not exhibit fluctuations above 3 GHz, while high quality pinches exhibited strong fluctuations in the 3-4 GHz range.

A synthetic E_z probe was placed in the simulated plasma, 0.75 cm from the axis. The synthetic probe from the pulsed power/circuit simulation exhibited its strongest fluctuations in the 3-4 GHz range (Figure 7b). Additionally, the simulated probe predicted higher frequency fluctuations that appear to be higher harmonics of the lower frequencies present. The two simulations with voltage wave driver also showed fluctuations in the same general frequency range, but with frequency peaks less aligned with the experimental data. This result may be expected, given that the rise of kinetic instabilities in the plasma could be heavily influenced by feedback from the driver. The simulations show fields of 10-40 T present for the entire pinch phase, corresponding to a lower hybrid frequency of ~ 4.6 -18 GHz. The observed oscillations are close to this frequency range and far from other characteristic plasma and cyclotron frequencies, suggesting that the long-suspected lower hybrid drift instability may be present.

A time-dependent inductance for the gun and plasma was calculated in the pulsed power/circuit simulation using the simulated magnetic energy and plasma current. The total inductance of the gun and plasma rises up to 10 nH during the ion beam formation and as high as 22 nH post-pinch. The contribution from the gun alone is 7 nH. A time-dependent resistance of the plasma was then calculated by dividing the component of the voltage which is not due to $d(LI)/dt$ by the plasma current. The plasma resistance is between 0.2 and 2 Ω during the fast ion beam formation, and rises up to 3.5 Ω post-pinch. The peak inductance and resistance values are higher than the 10-19 nH (7 nH gun + 3-12 nH plasma) and 1-1.5 Ω that we have estimated in our experiment from current traces¹⁵. They originate from an unphysically large dip in the current post-pinch. The current dip may be artificially high because the initialization of a vacuum region behind the sheath prevents a restrike from occurring in the

anode/cathode gap in these simulations. Future work will address the fidelity of the simulations after the pinch, so that post-pinch features such as restrikes and multiple pinches can be resolved.

Approximating the pinch plasma as a 1.1 cm long by 0.75 mm radius cylinder, a plasma resistance of 3.5 Ω implies a resistivity of 56 m Ω -cm. If we instead assume that the resistivity is closer to 1 Ω , as inferred from our current traces, then the implied plasma resistivity is 16 m Ω -cm. Classical resistivity from collisions and local plasma conditions in the pinch area is ~ 20 $\mu\Omega$ -cm, about 3 orders of magnitude lower than the anomalous resistivity observed in the simulations and experiment. The ion beam does not begin to form in the simulation until the resistivity is $> 100\times$ greater than classical values.

Summary

We have obtained simulated neutron yields and directly compared them with measured yields for two electrode geometries. The models with voltage wave driver predict neutron yields for the two geometries of 70-80% of their maximum measured yields and correctly rank the yields of the two similar guns. Inclusion of the driver characteristics at the boundary condition lowers the predicted neutron pulse length and total yield. Substantial agreement in ion beam energy distributions is found. We have made the first direct measurements of electromagnetic oscillations in a DPF plasma using an EM pick-up probe and shown that they exhibit similar frequency content to oscillations in simulated E_z fields. This correlation provides further evidence that a kinetic instability is responsible for pinch behavior and that fully kinetic simulations can reproduce this effect. This new simulation capability is well benchmarked at the kJ DPF level and now can be used to guide design of new DPF systems, including drivers.

Acknowledgements

This work performed under the auspices of the U.S. Department of Energy by Lawrence Livermore National Laboratory (LLNL) under Contract DE-AC52-07NA27344 and supported by the Laboratory Directed Research and Development Program (11-ERD-063) at LLNL. Computing support for this work came from the LLNL Institutional Computing Grand Challenge program.

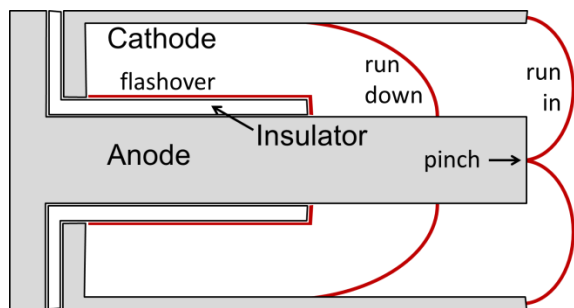


Figure 1: (Color online) Schematic of a dense plasma focus Z-pinch, including flashover, run-down, run-in, and pinch. The plasma sheath is shown in red (dark grey).

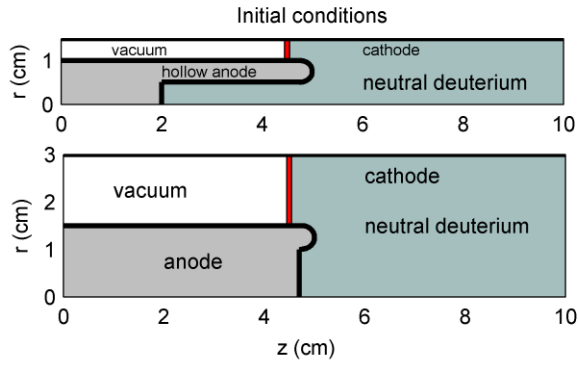


Figure 2: (Color online) Initial conditions for simulations of the two experimentally tested DPF guns. Plasma sheath of both ions and electrons is centered at $z = 4.5$. The region behind the sheath is vacuum. In front of the sheath is neutral deuterium gas.

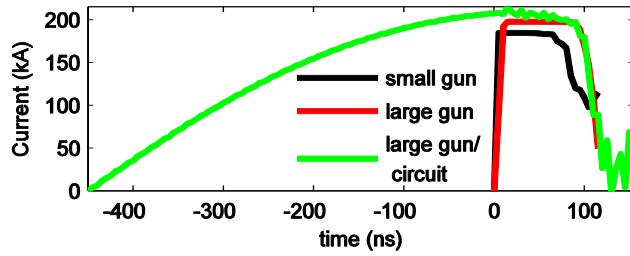


Figure 3: (Color online) Simulated plasma current as a function of time. The time at which particles are allowed to move is marked as $t=0$. Minor current oscillations in the pulsed power/circuit simulation appear when the particles are allowed to move, after the current has ramped up to its maximum value.

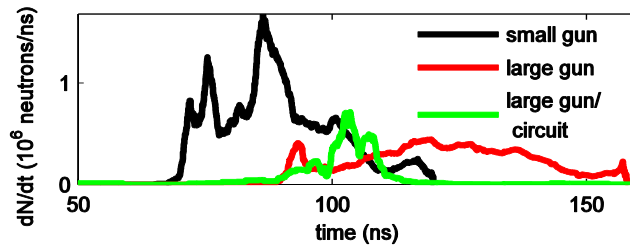


Figure 4: (Color online) Simulated neutron production rate as a function of time. Calculations remain stable and energy conserving throughout the entire pinch until after neutron production stops, allowing us to compare simulated yields from multiple electrode geometries.

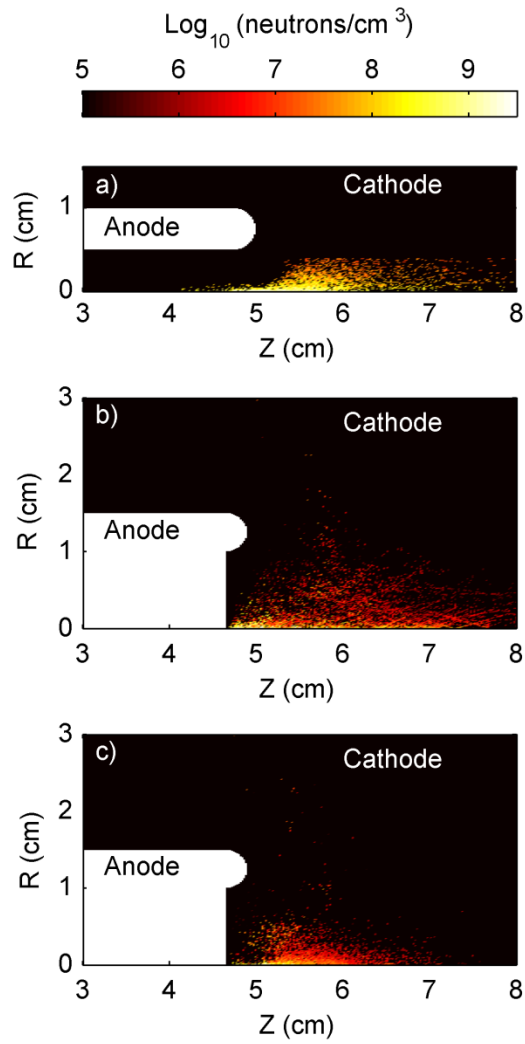


Figure 5: (Color online) Log of neutron density at neutron birth location for a) the smaller gun, b) the larger gun, and c) the larger gun with pulsed power circuit. The simulations predict that the majority of neutrons are born within 1 mm of the axis.

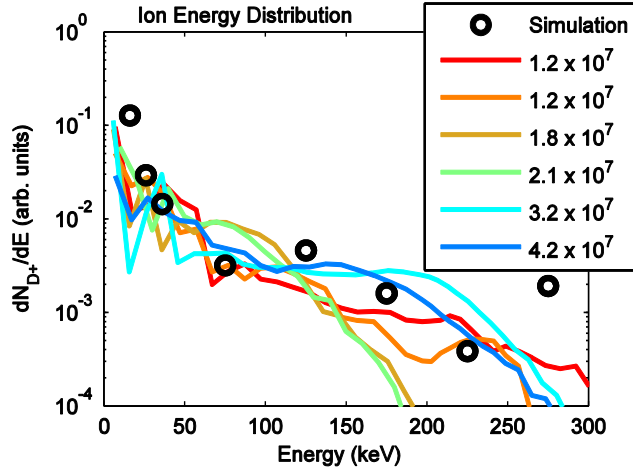


Figure 6: (Color online) Simulated (black circles) and measured (color) ion energy distributions for the smaller gun geometry. Shot yields are shown in legend and vary from 1.2×10^7 to 4.2×10^7 . Measured ion energy distributions have been obtained from time of flight Faraday cup measurements. In these shots, the Faraday cup signal is comparable to the noise for time of flight data corresponding to energies of ~ 300 keV and above.

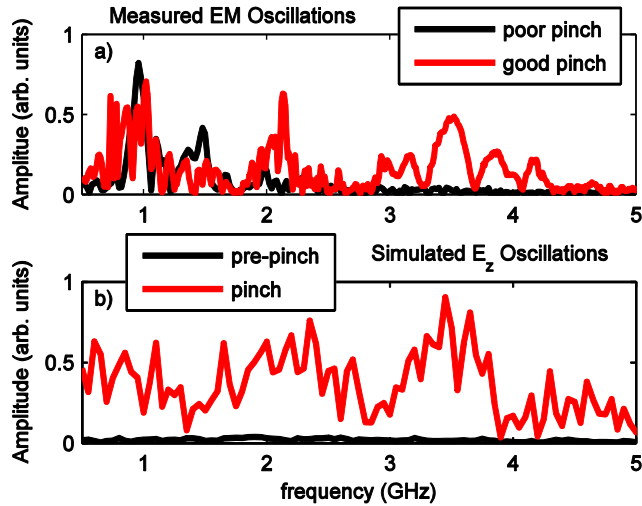


Figure 7: (Color online) Frequency content of measured EM oscillations (a) and simulated E_z probe (b) for the larger electrode configuration with full pulsed power circuit. Measured oscillations above 3 GHz are only observed in "high quality" pinches – those with large current dip and high neutron yield. Oscillations in the simulation are present during the pinch and for ~ 20 ns before the pinch. Both simulated and measured oscillations show activity in the 3-4 GHz range.

1. Bernard, A., H. Bruzzone, P. Choi, H. Chuaqui, V. Gribkov, J. Herrera, K. Hirano, A. Krejci, S. Lee, C. Luo, F. Mezzetti, M. Sadowski, H. Schmidt, K. Ware, C.S. Wong, and V. Zoita, *Scientific status of plasma focus research*. Journal of the Moscow Physical Society, 1998. **8**: p. 93-170.
2. Haines, M.G., *A review of the dense Z-pinch*. Plasma Physics and Controlled Fusion, 2011. **53**(9).
3. Mather, J.W., *INVESTIGATION OF THE HIGH-ENERGY ACCELERATION MODE IN THE COAXIAL GUN*. Physics of Fluids, 1964. **7**(11): p. S28-S34.
4. Mather, J.W., *FORMATION OF A HIGH-DENSITY DEUTERIUM PLASMA FOCUS*. Physics of Fluids, 1965. **8**(2): p. 366-&.
5. Deutsch, R., W. Kies, and G. Decker, *Theoretical-Model and Computer-Simulations of Electric Signals for Magnetically Driven Plasma Sheaths*. Plasma Physics and Controlled Fusion, 1986. **28**(12A): p. 1823-1839.
6. Gary, S.P. and F. Hohl, *Ion Kinematics in a Plasma Focus*. Physics of Fluids, 1973. **16**(7): p. 997-1002.
7. Haines, M.G., *Ion-Beam Formation in an $M = 0$ Unstable Z-Pinch*. Nuclear Instruments & Methods in Physics Research, 1983. **207**(1-2): p. 179-185.
8. Kondoh, Y. and M. Mamada, *Numerical Study on Charged-Particle Accelerations in the Plasma-Focus*. Physics of Fluids, 1986. **29**(2): p. 483-488.
9. Tang, V., M.L. Adams, and B. Rusnak, *Dense Plasma Focus Z-Pinches for High-Gradient Particle Acceleration*. Ieee Transactions on Plasma Science, 2010. **38**(4): p. 719-727.
10. Haruki, T., H.R. Yousefi, K. Masugata, J.I. Sakai, Y. Mizuguchi, N. Makino, and H. Ito, *Simulation of high-energy particle production through sausage and kink instabilities in pinched plasma discharges*. Physics of Plasmas, 2006. **13**(8): p. 082106.
11. Welch, D.R., D.V. Rose, R.E. Clark, C.B. Mostrom, W.A. Stygar, and R.J. Leeper, *Fully Kinetic Particle-in-Cell Simulations of a Deuterium Gas Puff z Pinch*. Physical Review Letters, 2009. **103**(25).
12. Schmidt, A., V. Tang, and D. Welch, *Fully Kinetic Simulations of Dense Plasma Focus Z-Pinch Devices*. Physical Review Letters, 2012. **109**(20): p. 205003.
13. Gerdin, G., M.J. Tanis, and F. Venneri, *Observation of Microwave Emission from a Plasma-Focus at Frequencies Well Below the Mean Plasma Frequency*. Plasma Physics and Controlled Fusion, 1986. **28**(3): p. 527-545.
14. Welch, D.R., D.V. Rose, M.E. Cuneo, R.B. Campbell, and T.A. Mehlhorn, *Integrated simulation of the generation and transport of proton beams from laser-target interaction*. Physics of Plasmas, 2006. **13**(6): p. 063105.
15. Ellsworth, J.L., S. Falabella, V. Tang, A. Schmidt, G. Guethlein, S. Hawkins, B. Rusnak, *Design and Initial Results from a Kilojoule Level Dense Plasma Focus with Hollow Anode and Cylindrically Symmetric Gas Puff*. Review of Scientific Instruments, 2014. **85**.
16. Decker, G., W. Kies, M. Malzig, C. Vancalker, and G. Ziethen, *High-Performance 300 kV Driver Speed 2 for MA Pinch Discharges*. Nuclear Instruments & Methods in Physics Research A, 1986. **249**(2-3): p. 477-483.
17. Kies, W., *Power Limits for Dynamic Pinch Discharges*. Plasma Physics and Controlled Fusion, 1986. **28**(11): p. 1645-1657.
18. Decker, G., W. Kies, and G. Pross, *The 1st and the Final 50 Nanoseconds of a Fast Focus Discharge*. Physics of Fluids, 1983. **26**(2): p. 571-578.
19. Bostick, W.H., H. Kilic, V. Nardi, and C.W. Powell, *Time-Resolved Energy-Spectrum of the Axial Ion-Beam Generated in Plasma-Focus Discharges*. Nuclear Fusion, 1993. **33**(3): p. 413-420.

20. Gullickson, R.L. and H.L. Sahlin, *MEASUREMENTS OF HIGH-ENERGY DEUTERONS IN PLASMA-FOCUS DEVICE*. Journal of Applied Physics, 1978. **49**(3): p. 1099-1105.